Direct Nondestructive Imaging of Magnetization in a Spin-1 Bose-Einstein Gas

J. M. Higbie, L. E. Sadler, S. Inouye, A. P. Chikkatur, S. R. Leslie, K. L. Moore, V. Savalli, and D. M. Stamper-Kurn
Department of Physics, University of California, Berkeley, California 94720, USA
(Received 18 February 2005; published 26 July 2005)

Polarization-dependent phase-contrast imaging is used to resolve the spatial magnetization profile of an optically trapped ultracold gas. This probe is applied to Larmor precession of degenerate and nondegenerate spin-1 ^{87}Rb gases. Transverse magnetization of the Bose-Einstein condensate persists for the condensate lifetime, with a spatial response to magnetic field inhomogeneities consistent with a mean-field model of interactions. In comparison, the magnetization of the noncondensed gas decoheres rapidly. Rotational symmetry implies that the Larmor frequency of a spinor condensate be density independent, and thus suitable for precise magnetometry with high spatial resolution.

DOI: 10.1103/PhysRevLett.95.050401 PACS numbers: 03.75.Gg, 05.30.Jp, 52.38.Bv

Quantum fluids with a spin degree of freedom have been of long-standing interest, stimulated both by the complex phenomenology of superfluid ^{3}He [1] and by p-wave superconductivity [2]. Measurements of magnetization and magnetic resonance have been crucial to revealing the internal structure of these systems, inviting the application of such techniques to related fluids. Advances in ultracold atomic physics have now led to the creation of novel multicomponent quantum fluids including pseudospin-$\frac{1}{2}$ Bose-Einstein condensates (BECs) [3] and spin-1 and -2 condensates of Na [4,5] and ^{87}Rb [6–8].

The internal state of a multicomponent system is characterized by the populations in each of the components and the coherences among them. However, in all previous studies of the spin-1 or spin-2 spinor condensates, while the populations in each magnetic sublevel were measured, no information was obtained regarding the coherences between overlapping populations [4,6–10]. Moreover, although spatial patterns of longitudinal magnetization have been reconstructed from images of freely expanding spinor gases, the expansion process limits the resolution obtainable [9,11,12].

In this Letter, we exploit atomic birefringence to image the magnetization of an ultracold spin-1 Bose gas nondestructively with high spatial resolution. By varying the orientation of an applied magnetic field with respect to our imaging axis, we measure either longitudinal magnetization, which derives from the static populations in each of the magnetic sublevels, or transverse magnetization, which derives from time-varying $\Delta m = 1$ coherences. This probe is used to observe Larmor precession in both degenerate and nondegenerate spinor Bose gases. In particular, optical characterization of Larmor precession in a BEC provides a novel probe of the relative phases between condensates in different internal states with excellent temporal and spatial resolution (see Refs. [13] for other recent measurements of the condensate phase). Moreover, the long coherence times we observe in the presence of magnetic inhomogeneity and the density independence of the Larmor-precession frequency (see below), make this system very promising for high-resolution magnetometry.

This work is related to experiments by the JILA group in which either continuous [14] or pulsed [12] microwave fields were used to analyze a two-component (pseudospin-$\frac{1}{2}$) ^{87}Rb gas. However, in contrast to this pseudospin system, the spin-1 spinor gas has a richer state space, displays actual magnetization, and possesses vector symmetry, implying rotationally invariant interactions. This invariance manifests itself in our work in the gapless nature of ''magnon'' excitations, and in the density independence of the Larmor-precession frequency.

Our probe relies on the phase-contrast technique, which permits multiple-shot *in situ* imaging of optically thick samples [15]. One can thus directly observe the dynamics of a single gaseous sample, rather than reconstructing them from experiments on many different samples. The phase-contrast imaging signal strength for polarized probe light depends on both the density and the internal state of the atoms being imaged. In the case of imaging an $F = 1$ gas of ^{87}Rb with σ_+ circularly polarized light near the $F = 1 \rightarrow F' = 2$ $D1$ transition, the phase-contrast signal, calculated from the relevant phase shifts with reference to the Clebsch-Gordon coefficients in Fig. 1, is $\frac{1}{4}\tilde{n}\sigma(\gamma/2\delta) \times (1 + \frac{5}{6}\langle F_y\rangle + \frac{1}{6}\langle F_y^2\rangle)$ assuming that the optical susceptibility of the dilute gas is small. Here $\tilde{n}$ is the column density, $\sigma = 3\lambda^2/2\pi$ the resonant cross section, $2\delta/\gamma$ the probe detuning in half linewidths, and F_y the projection of the dimensionless atomic spin on the probe axis. The phase-contrast signal is thus largely a local measure of one vector component of the magnetization, when the density is known. Other components of the magnetization and the magnetic quadrupole (''nematicity'') may be extracted by magnetic field rotations and by changing polarization and detuning, potentially allowing complete reconstruction of the single-particle density matrix [16]. Here, the magnetization signal only is considered, though the probe is slightly sensitive to nematicity through the $\langle F_y^2\rangle$ dependence of the phase-contrast signal.

We perform our experiments by collecting 5×10^9 ^{87}Rb Zeeman-slowed atoms in a magneto-optical trap, loading them into a Ioffe-Pritchard magnetic trap, and

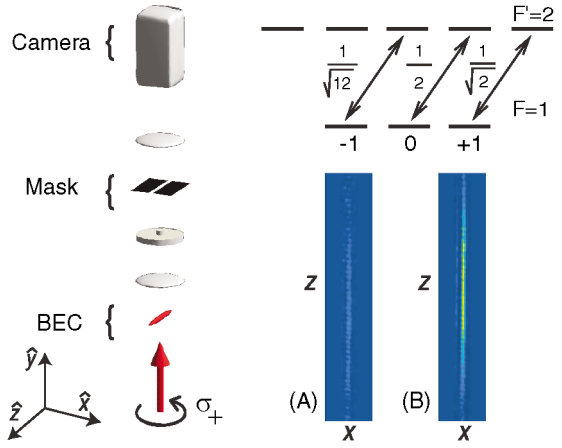

FIG. 1 (color). Imaging system for direct detection of atomic magnetization. Left: Circularly polarized probe light illuminates the trapped gas. A first lens and phase plate form a primary phase-contrast image which is selectively masked and then reimaged by a second lens onto the camera as one of ~40 frames which form a single composite image. Top right: Clebsch-Gordan coefficients for the imaging transition. Bottom right: Sample images of a BEC (a) with the atomic spin along $-\hat{y}$ and (b) with the spin along $+\hat{y}$, demonstrating the magnetization sensitivity of our technique.

evaporatively cooling to ~2 μK, before transferring the atoms into a single-beam, linearly polarized optical dipole trap (ODT). The ODT derives from a free-running 825 nm diode laser, whose fiber-coupled output is focused to diffraction-limited beam waists of $(w_x, w_y) = (39, 13)$ μm at the trap. For the condensate studies, the ODT power is then ramped down over 700 ms from 12 mW to a final value of 2.3 mW, corresponding to trap frequencies $(\omega_x, \omega_y, \omega_z) = 2\pi(150, 400, 4)$ s^{-1} (axis orientations are indicated in Fig. 1). The resulting evaporation yields nearly pure condensates of 4×10^6 atoms with a peak density of 5×10^{14} cm^{-3}. For the studies of the thermal cloud, we hold the ODT power at 6.4 mW, yielding a gas of $\sim 6 \times 10^6$ atoms at a temperature of 1.1 μK, and a trap with frequencies $(\omega_x, \omega_y, \omega_z) = 2\pi(250, 670, 7)$ s^{-1}.

The atomic sample is phase-contrast imaged (total magnification $\times 12$) onto a CCD camera. A physical mask blocks illumination of all but a narrow slit-shaped region of the CCD chip. With a rapid frame-shifting mode of our camera, we record 40 consecutive images, each 25 pixels wide, at a rate of 20 kHz. We use probe light detuned 212 MHz below the $F = 1 \rightarrow F' = 2$ $D1$ transition ($\lambda = 795$ nm). Probe pulses are 5 μs long with an average intensity of 300 μW/cm^2 [17].

We induce Larmor precession in our atomic sample starting with a spin-polarized gas in the $|F = 1, m_F = -1\rangle$ state and a bias field of 54 ± 2 mG transverse to the probe [18]. A resonant rf pulse tips the spin vector by an angle $\theta \simeq \pi/2$. As the tipped spin precesses about the bias field, the phase-contrast image intensities oscillate [Fig. 2(a)]. We extract the peak signal from each of the 40 phase-contrast images by first binning in the $\hat{z}$ direction over a small region (27 μm for the BEC and 108 μm for the thermal cloud) at the center of the cloud, and then fitting to a sinc function in the radial ($\hat{x}$) direction to account for aberrations arising from imaging objects near the 6 μm imaging resolution limit. The temporal oscillation in the peak height of our phase-contrast images is clearly visible [Fig. 2(b)], and is present only after the rf pulse is applied. The transverse magnetization signals can be compared to those from the static *longitudinal* polarization of spin-polarized samples in the $|F = 1, m_F = \pm 1\rangle$ states held in a magnetic field pointing along the imaging axis (Fig. 1). This comparison confirms that the Larmor-precessing samples are maximally magnetized. We note that the ratio of 4.2 observed between the signals from spin-up and spin-down atoms is less than the theoretical value of 6, perhaps because of imperfect probe polarization.

The Larmor frequency of ~38 kHz is chosen in order to maintain accurate control of the field direction and avoid unwanted spin flips due to low-frequency field noise in our laboratory. Since twice the 20 kHz frame rate of our images is within ~2 kHz of the Larmor frequency, we observe an aliased low-frequency oscillation at the difference fre-

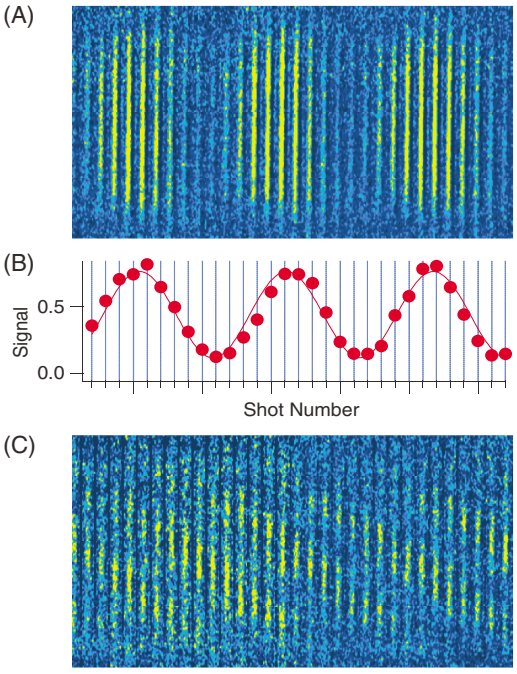

FIG. 2 (color). Direct imaging of Larmor precession of a spinor BEC through magnetization-sensitive phase-contrast imaging. Shown are 31 consecutive images each with 325 × 18 μm field of view. (a) Larmor precession is observed as a periodic modulation in the intensities of repeated images of a single condensate. (b) The peak signal strength oscillates at a rate which results from aliased sampling of a precisely measured 38.097(15) kHz Larmor precession at a sampling rate of 20 kHz. (c) In the presence of an 8 mG/cm axial gradient, images indicate "winding" of the transverse magnetization along the condensate. Images begin (a) 24.5 ms or (c) 14.5 ms after the tipping rf pulse. In (a), the field gradient is cancelled to less than 0.2 mG/cm.

quency. Combined with the less precise, but absolute, determination of the rf pulse resonance frequency, the Larmor-precession signal measures in a single shot the instantaneous magnetic field to a fraction of a milligauss.

The amplitude of the Larmor-precession signal gives a quantitative measure of the coherences among Zeeman sublevels. Atomic gases with long-lived and well-characterized coherences have important scientific and technological applications, from precision measurements of weak interactions to atomic clocks and magnetometers. The lifetime of magnetic-field-insensitive hyperfine coherences in ultracold atoms has been studied [11,19,20], with coherence times up to 2 s reported. To measure the lifetime of *Zeeman* coherences in an ultracold Bose gas, we tip the atomic spin using an rf pulse, as before, and then wait a variable time before measuring the amplitude of the Larmor-precession signal (the ''tip and hold'' method). To isolate effects that specifically diminish transverse magnetization from atom-number loss or other systematic effects, we alternatively reverse the order of the delay and the rf pulse (''hold and tip'').

Results of such a measurement are shown in Fig. 3 [21]. The lifetime of transverse magnetization in a spinor BEC, taken as the $1/e$ time of an exponential fit to the precession amplitude vs time, was 670 ± 120 ms, compared to the measured 830 ± 120 ms condensate lifetime (determined from the hold and tip method) in the optical trap. Thus, the BEC remains fully magnetized, even in the presence of interparticle interactions and of magnetic field inhomogeneity (discussed below). No significant decoherence occurs other than that attributable to overall number loss, consistent with 3-body decay [22]. We note that on other repetitions of the experiment (data presented in Fig. 4), decoherence was observed on a time scale of about 400 ms, somewhat shorter than the condensate lifetime. We cannot presently account for this variation.

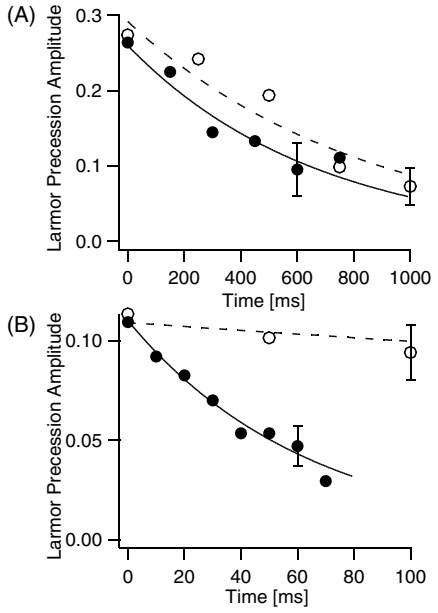

FIG. 3. Decay of the Larmor-precession amplitude for (a) a BEC and (b) a thermal cloud. Data from the tip and hold (filled circles) or hold and tip (open circles) methods are compared (see text). The $1/e$ decay time of Larmor precession in a BEC was 670 ± 120 ms, close to that of the hold and tip signal (830 ± 120 ms), indicating no decoherence source other than number loss. The 65 ± 10 ms decay time of Larmor precession in a thermal cloud was an order of magnitude shorter than that of the hold and tip signal (1100 ± 500 ms).

As the condensate is held for long times after the magnetization is tipped into the transverse plane, the Larmor-precession signal begins to display a position-dependent phase shift (observed up to 25 rad) along the condensate axis, resulting from magnetic inhomogeneity [Fig. 2(c)]. For example, a gradient of the field magnitude along the long axis of the condensate leads to a ''corkscrew'' magnetization, which winds up over time (similar observations were made of pseudospin-$\frac{1}{2}$ spinor condensates [14]). Qualitatively, the condensed gas behaves as if its constituent atoms were frozen in place, precessing at a frequency given by the local value of the inhomogeneous magnetic field.

The evolution of transverse condensate magnetization can be described by the separate motion of each of the three magnetic components. In a frame rotating at the Larmor frequency, this magnetization is quasistatic. A magnetic field gradient imposes, over short times, a e^{imqz} relative phase (or imparts a $m\hbar q$ relative momentum) on the three components, labeled by the magnetic quantum number m. This defines a helical magnetization with pitch $2\pi/q$. At longer times, the trapping potential and condensate density begin to influence the motion of the separate components, and hence the magnetization. For example, in a harmonically confined *noninteracting* spinor BEC, one would expect the magnetization to rephase along the length of the BEC after one trapping period. However, we observe no such dynamics, finding the phase of Larmor precession at different portions of the condensate to advance linearly with time through the 250 ms axial trap period. This behavior, at least for the case of small gradient, can be

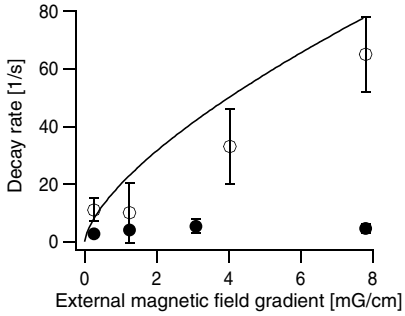

FIG. 4. Dependence of Larmor-precession decay rate on applied gradient [27]. Decay rates for the condensate are represented by filled circles and for the thermal cloud by open circles. The solid curve is a theoretical prediction for the thermal-cloud precession decay rate, as discussed in the text.

explained by noting that slight rotations of the magnetization are associated with magnons possessing a gapless and free-particle-like spectrum above the chemical potential, which is constant across the condensate [23]. Thus, for an *interacting* spinor condensate, the combined effect of the inhomogeneous condensate mean-field energy and the trap potential is to cause magnons, or small-scale magnetization rotations, to advance as if no external potential were present. We expect this argument to apply also to larger rotations of the magnetization, in accordance with our observations.

In contrast, transverse magnetization in a nondegenerate spinor gas decays much faster than that in a BEC (Fig. 3). Moreover, while the (local) Zeeman coherence in a BEC appears unaffected by magnetic inhomogeneity, the decoherence rate in a thermal gas depends strongly on the applied magnetic gradient (Fig. 4). The thermal-cloud Zeeman decoherence rates are estimated simply as $\Gamma_{\mathrm{LP}} = (\Omega_{\mathrm{L}}'^2 v_{\mathrm{th}}/\pi^2 n \sigma_c)^{1/3}$, where $\Gamma_{\mathrm{LP}}^{-1}$ is the time for an atom to diffuse [24] into a field large enough to dephase its spin by π relative to a stationary spin, v_{th} is the mean thermal velocity, n the number density, σ_c the collisional cross section, and $2\hbar\Omega_{\mathrm{L}}'/\mu_{\mathrm{B}}$ the magnetic gradient. This simple result is shown in Fig. 4 to agree fairly well with measurement. We note that this picture neglects spin waves, which were observed in pseudospin-$\frac{1}{2}$ gases [11,12,25] and which should exist (in modified form) in spin-1 Bose gases as well.

The demonstrated ability to image directly the magnetization of a spinor Bose gas and the observation of long-lived Zeeman coherences point to a number of future investigations. Given the quadratic dependence of the dominant 3-body loss rate on condensate density, much longer Zeeman coherence times may be attained in lower-density spinor BECs. Furthermore, one expects the Larmor-precession frequency of a spinor BEC to be density independent at low magnetic fields. This result stems from the vectorial symmetry of the atomic spin, which requires the zero-field interatomic interactions to be rotationally invariant [23]. Consequently, spinor BECs constitute an attractive system for precise magnetometry with high spatial resolution (~ 10 μm). Moreover, such magnetometry may be regarded as a form of condensate-based interferometry, resolving *spatially varying* phase relations among *three* condensed components.

Our imaging method also promises to illuminate the mostly unexplored properties of spinor condensates. For example, spin-1 condensates of ^{87}Rb are predicted to be ferromagnetic [23,26]. While measurements of populations of the magnetic sublevels are consistent with this prediction [6,7], no information on coherences, and thus no conclusive evidence of ferromagnetism, has been obtained. We are presently attempting to detect the spontaneous Larmor precession of a ^{87}Rb condensate as it relaxes to a ferromagnetic ground state. These experiments will be described elsewhere.

We thank F. Lienhart, M. Pasienski, E. Crump, and the UCB Physics Machine and Electronics Shops for assistance, and W. Ketterle and D. Budker for helpful comments. This work was supported by the NSF, the Hellman Faculty Fund, and the Alfred P. Sloan and the David and Lucile Packard Foundations. K. L. M. acknowledges support from the NSF and S. R. L. from the NSERC.

[1] D. Vollhardt and P. Wölfle, *The Superfluid Phases of Helium 3* (Taylor & Francis, New York, 1990).
[2] A. P. Mackenzie and Y. Maeno, Rev. Mod. Phys. **75**, 657 (2003).
[3] D. S. Hall *et al.*, Phys. Rev. Lett. **81**, 1543 (1998).
[4] J. Stenger *et al.*, Nature (London) **396**, 345 (1998).
[5] A. Görlitz *et al.*, Phys. Rev. Lett. **90**, 090401 (2003).
[6] H. Schmaljohann *et al.*, Phys. Rev. Lett. **92**, 040402 (2004).
[7] M.-S. Chang *et al.*, Phys. Rev. Lett. **92**, 140403 (2004).
[8] T. Kuwamoto *et al.*, Phys. Rev. A **69**, 063604 (2004).
[9] H.-J. Miesner *et al.*, Phys. Rev. Lett. **82**, 2228 (1999).
[10] D. M. Stamper-Kurn *et al.*, Phys. Rev. Lett. **83**, 661 (1999).
[11] H. J. Lewandowski *et al.*, Phys. Rev. Lett. **88**, 070403 (2002).
[12] J. M. McGuirk *et al.*, Phys. Rev. Lett. **89**, 090402 (2002).
[13] Y. J. Wang *et al.*, Phys. Rev. Lett. **94**, 090405 (2005); M. H. Wheeler *et al.*, Phys. Rev. Lett. **93**, 170402 (2004); M. Saba *et al.*, Science **307**, 1945 (2005).
[14] M. R. Matthews *et al.*, Phys. Rev. Lett. **83**, 3358 (1999).
[15] M. R. Andrews *et al.*, Phys. Rev. Lett. **79**, 553 (1997).
[16] I. Carusotto and E. J. Mueller, J. Phys. B **37**, S115 (2004).
[17] Probe light at 300 μW/cm^2 imparts state-dependent ac Stark shifts equivalent to a 0.6 mG field along the probe direction. We observed no spin flips or number loss from our sample from this pulsed field.
[18] After nulling the magnetic field to <5 mG, we apply additional fields either along or orthogonal to the imaging axis. Remaining field fluctuations cause shot-to-shot rms variations of 1.6 kHz in the Larmor-precession frequency.
[19] D. M. Harber *et al.*, Phys. Rev. A **66**, 053616 (2002).
[20] N. Davidson *et al.*, Phys. Rev. Lett. **74**, 1311 (1995).
[21] Amplitudes are averaged over three independent, contiguous 27 μm regions.
[22] E. A. Burt *et al.*, Phys. Rev. Lett. **79**, 337 (1997).
[23] T.-L. Ho, Phys. Rev. Lett. **81**, 742 (1998); T. Ohmi and K. Machida, J. Phys. Soc. Jpn. **67**, 1822 (1998).
[24] Because of the large collision rate (200 Hz) compared with the axial oscillation frequency (7 Hz), thermal atoms move diffusively and slower than they would ballistically; also noted in Ref. [19].
[25] N. P. Bigelow *et al.*, Phys. Rev. Lett. **63**, 1609 (1989).
[26] N. N. Klausen *et al.*, Phys. Rev. A **64**, 053602 (2001).
[27] For Fig. 4 we used the Larmor phase gradient measured in a BEC to ascertain the axial field gradient to better than 0.2 mG/cm, a curvature of about 20 mG/cm^2 then becoming dominant.